

Review of the recent x-ray and neutron powder diffraction studies on lead zirconate titanate

J. Frantti

*Laboratory of Physics, Helsinki University of Technology, P.O. Box 4100, FIN-02015 HUT, Finland**

(Dated: December 2, 2024)

The issues related to the structure refinement of $\text{Pb}(\text{Zr}_x\text{Ti}_{1-x})\text{O}_3$ (PZT) solid solutions are discussed. Particular attention is paid on the modelling of the co-existing phases in the vicinity of the morphotropic phase boundary (MPB), where local symmetry is often significantly lower than the average symmetry. As recent studies reveal, two-phase co-existence in the vicinity of the MPB is a thermodynamical necessity. Significantly different structural models for PZT with x in the vicinity of the MPB have recently been published. Structural models, based on x-ray, neutron and electron diffraction studies, are reviewed and two essentially different approaches were identified: (i) a method where space group symmetry was decreased until the features due to the local distortions were 'modelled' and (ii) a method where the highest space group symmetry compatible with the powder diffraction data was used together with a model for a local disorder. Related to the method (ii), the essential features of a model taking the hkl -dependent line broadening into account are summarized. The underlying theme is to consider how local regions, with symmetry lower than the average symmetry, should be modelled. Method (i) often introduces unjustified structural parameters and should be avoided. By studying the temperature and composition dependence of the structural parameters (and phase fractions in the case of the two phase samples) one can further test the proposed models. The connection between the structure and piezoelectric properties, with emphasis on the co-existence of the rhombohedral and monoclinic phases, is discussed in light of the recent first-principles computational studies. Also problems connected to sample preparation and data collection are pointed out.

PACS numbers: 77.84.Dy 61.12.Ld 61.50.Ah 81.30.Dz

I. INTRODUCTION

Lead zirconate titanate $[\text{Pb}(\text{Zr}_x\text{Ti}_{1-x})\text{O}_3]$, (PZT)] solid solutions are among the most widely used ferroelectric ceramics. The importance of PZT ceramics with morphotropic phase boundary (MPB) compositions is due to the exceptionally good piezoelectric properties they exhibit¹, which in turn has motivated numerous studies seeking physical mechanisms responsible for this extraordinary behaviour (for a review of the various studies see ref.²). Crystal structure studies and the changes in atomic positions versus composition, temperature, pressure or electric field have a central role for the understanding of these materials: nuclei positions, together with the electron density, determine the electric polarization vector on which the numerous applications are based on. It is essential to understand how the polarization vector changes as a function of electric field, composition, temperature or pressure. Qualitatively, the average structural tendencies versus composition, temperature or pressure of ionic compounds, such as PZT, can be understood by considering the Madelung energies which decreases with decreasing crystal volume until the shortrange interactions balance the crystal volume to its equilibrium value. For ionic crystals the contribution of Madelung energy to the total energy is dominant and implies that crystal volume tends to be minimized. By tilting the oxygen octahedra the crystal can partially compensate for the effect of a larger average B -cation (Zr and Ti) size which increases with increasing Zr content

x . This is seen from the behaviour of Zr rich samples: once crystal adopts $R3c$ symmetry, instead of $R3m$ symmetry, the volume per primitive cell is smaller. This is consistent with the notion that in the case it would cost a lot of energy to contract the oxygen octahedra (due to the shortrange interactions which limit the compression of octahedra) overall energy gain can still be obtained by tilting the oxygen octahedra. Typically the changes in octahedral tilts occur consistently versus composition³ or temperature⁴ and thus particular care is necessary before anomalous octahedral tilt systems are considered. Secondly, in the case of PZT (and other Pb containing perovskite ferroelectrics) the crystals suffer from numerous defects. Nevertheless, these defects do have a significant role for ferroelectricity. An example is provided by the Pb ions which are significantly displaced from their ideal sites and which respond to the external electric field or pressure by adjusting their position with a corresponding changes in polarization vector^{5,6}. Similar consideration holds for Zr and Ti, whose positions are disordered in two ways: (i) the probability that the B -cation site is occupied by Zr (Ti) is x ($1-x$) and (ii) the fractional coordinates of Zr and Ti are different. The confirmation of the assumption (i) is not straightforward, but various powder diffraction and Raman scattering studies show that it is a good approximation for most cases. By high resolution powder diffraction instruments it is possible to study these peculiar features by extracting information from the line shapes, in addition to the determination of the average structure. However, it became apparent that a rather complex lineshape is necessary for the modelling of

the diffraction peak profiles, for examples see refs.⁷ and⁸. The structure of the PZT ceramics with composition in the vicinity of the MPB are notoriously tricky to model. There are two main reasons for that: (i) in practice, no single phase samples are obtained, instead one observes two perovskite phases and (ii) diffraction peak profiles are rather complex. Both factors are connected to the fact that this 'boundary' separates tetragonal and rhombohedral phases which do not possess a group-subgroup relationship. The experimental observation that monoclinic *Cm* phase separates tetragonal (space group *P4mm*) and rhombohedral (at room temperature space group is *R3m*) phases clarified the situation: *Cm* is a common subgroup of *P4mm* and *R3m* phases^{5,6}. Correspondingly, instead of morphotropic phase boundary one occasionally refers to morphotropic phase^{5,6}. Thus, it is not a surprise that the structural disorder is particularly pronounced in the vicinity of MPB. This is also partially due to fact that typically the structure and composition of the grain boundaries and bulk are different. This is revealed from the Bragg reflection line shapes, which are almost 'Gaussian' like at room temperature^{6,9} in the case of the less abundant phase. Even though it is still an open question whether *Cm* is stable phase in PZT system it provides an explanation to the peak value of piezoelectric constant via the polarization rotation theory: first-principles computations demonstrated that the polarization rotation provides the lowest free energy path along which there is a large coupling between the polarization and the electric field¹⁰, consistently with the experimentally observed large electromechanical response.

Recently, a model which used two monoclinic phases (space group symmetries *Cc* and *Cm*) was claimed to be the correct low-temperature structure of PZT with $x \approx 0.52^{11}$, see also note¹² and refs.^{13,14}. This report stated that *R3c* symmetry is not a correct choice for PZT with $x \approx 0.52^{11}$. The fact that superlattice reflections allow the distinction of *R3c* and *Cc* symmetries in favour of the former was overlooked in this study. Nevertheless, *Cc* symmetry predicts reflections well isolated from those of the *R3c* symmetry. To summarize the models proposed in refs.^{11,13}, we note that the phase which traditionally has been assigned to the rhombohedral symmetry¹, was assigned to *Cm* symmetry and space group symmetry *P4mm* (at room temperature) or *Cc* (at low temperature) was assigned to the phase which was modelled by *Cm* symmetry in refs.^{4,5,6}. Thus, significant changes to the well known PZT phase diagram¹ were proposed. To understand the problems related to such a model (abbreviated as *Cc + Cm*) and the reason why the use of space group *Cc* was previously rejected⁴ it is necessary to summarize the crucial role of the local disorder resulting in *hkl*-dependent line broadening¹⁵. Erroneous space group symmetry assignments likely result in once this line broadening is compensated for by reducing the space group symmetry¹⁶. The *hkl*-dependent line broadening is an inherent property of PZT powders due to the local distortions, and is already seen in tetragonal Ti rich com-

positions and even at high temperature cubic phase¹⁷. Namely, the Bragg reflection widths were anisotropic already at the cubic phase, although the linewidths were an order of magnitude smaller than in the case of the low-temperature phases. It is well known that broad peaks are observed in Raman spectra collected at high temperature cubic phase, even though no first order Raman scattering is allowed for ideal symmetry. For example, see ref.¹⁸, where the modes appearing in cubic phase were assigned to the first order scattering, activated by the local disorder, by studying the temperature dependence of the intensities. The same behaviour was observed in a closely related $\text{Pb}(\text{Hf}_x \text{Ti}_{1-x})\text{O}_3$ (PHT) system with $0.10 \leq x \leq 0.40$, where the peak widths of the $00l$ reflections were twice as large as the widths of $h00$ reflections¹⁹. It must be emphasized that no signs of symmetry lowering from the *P4mm* symmetry was observed in this high-resolution neutron powder diffraction study. In contrast, light scattering experiments revealed that both in the case of tetragonal PZT and PHT samples deviations from the average symmetry were observed^{20,21,22}. Namely, the number of Raman active modes was larger than the symmetry found by diffraction techniques would allow. Once the diffraction patterns were examined it became apparent that there was no justification to use lower space group symmetry. A model based on lower space group symmetry would simply result in physically meaningless structural parameters. In this case, the essential point was that even if one insist to invoke lower space group symmetry in order to explain the observed Raman spectra the changes in bond lengths should be so large that also high resolution neutron powder diffraction patterns should reveal it. Although one can decrease the average symmetry to decrease the residuals, a more realistic model is obtained by assuming that (i) the *average symmetry* over a length scale of a few hundred nanometers is *P4mm*, and (ii) deviations from this symmetry occur in a local scale (of a few unit cells). The essential point here is that these deviations are not periodical, at least not in a scale probed by x-ray or neutron diffraction. However, ion displacements (particularly those of Pb ions) are likely correlated in a scale of a few unit cells².

Transmission electron microscopy (TEM) and electron diffraction (ED) studies revealed extra reflections in rhombohedral PZTs²³. The origin of these reflections was more recently studied by TEM and ED together with neutron powder diffraction (NPD) techniques²⁴. In this study superlattice reflections of the type *R*₁, *R*₂, *M*₁ and *M*₂ (see Table I in ref.²⁴) were observed, consistently with ref.²³. Among these reflections only *R*₂ is consistent with *R3c* symmetry²⁴. We summarize the observations and interpretations given in ref.²⁴ as follows: (i) *M*-type reflections were accompanied by satellites, (ii) different areas in the same grain resulted in changes in the relative intensities of the superlattice reflections so that in some cases the extra spots completely disappeared, (iii) by collecting data on samples prepared from single crystals and

ceramics it was found that the satellites around M points are characteristic feature of only ceramics, (iv) by studying the temperature dependence of the extra reflections they could be assigned to the ferroelectric state (no extra reflections were observed at cubic phase), (v) octahedral tilts and distortions alone are insufficient to explain R_1 and M superlattice reflections *with the intensities observed* (it was demonstrated that very weak superlattice reflections could be obtained using unrealistically large oxygen octahedra tilts and distortions), and (vi) NPD experiments revealed *only* R_2 reflections, consistently with an average $R3c$ symmetry. To explain these observations models based on locally ordered regions presenting antiparallel cation displacements were proposed (see also ref.³ where structural models based on NPD experiments were given) and compared with experiments. Finite size effect was proposed as an underlying reason for the phenomena observed by TEM and ED techniques. This is an important point since it suggests that *these puzzling phenomena, observed by TEM and ED techniques, do not occur in the case of bulk ceramics*. However, the tendency of Pb ions to form four short bonds with oxygen is a feature observed through NPD studies³. This tendency is also seen from the models constructed to explain the observed ED patterns²⁴. It is also worth to note that similar conclusions were obtained through Monte Carlo simulations reported in ref.²⁵: M -like superlattice reflections are not present in pure bulk crystals but might be locally induced by surfaces over some range of temperature.

After a reasonable model for local distortions or locally ordered regions is identified a selection of an appropriate instrument for the (preferably neutron) powder diffraction experiments to further test the structural models is essential. For example, the Cm phase was identified by studying the peak split of the pseudo-cubic 110 reflections^{5,6} through high resolution synchrotron experiments. This peak split was beyond the resolution of the instrument used in ref.¹¹ and there is no way to recover the lost information. Thus, new refinements do not compensate for the problems connected to the low-resolution data collected with insufficient counting time. The role of the spatial composition variation (which in practice cannot be eliminated) in the vicinity of the phase boundary is an old and still a valid explanation for the two phase 'co-existences' and also largely explains the hkl -dependent line broadening. A qualitative model which was constructed by studying changes in structures and their mutual phase fractions versus temperature and x was proposed in refs.⁴ and¹⁷. These aspects are reviewed below. In section II we discuss the role of the spatial composition variation on the PZTs with x in the vicinity of the MPB, as it is closely connected to the two phase co-existence. The main goal of the section II is to provide an explanation for the different type of domains by taking into account the recent thermodynamical considerations and to show that these ideas are consistent with numerous experimental observations. Anisotropic

line broadening is discussed in section III. Section IV reviews different two-phase models proposed for PZT in the vicinity of MPB. Section V summarizes the results obtained through bond-valence computations and recent computational studies.

II. SPATIAL COMPOSITION VARIATION

The PZT system is frequently assumed to be a binary solid solution of $PbTiO_3$ and $PbZrO_3$ *without solubility gaps*, as was summarized in ref.²⁶. According to ref.²⁶, once a solid solution is formed at high temperature (typically above $800^\circ C$), the chemical composition cannot be changed at low temperatures, but the system can have temperature-induced *diffusionless* structural phase transitions. The validity of this assumption has been questioned in refs.^{27,28} and it was reported that PZT solutions exhibit a positive enthalpy of mixing that suggests *a tendency towards immiscibility and phase decomposition*. Thus, it was proposed²⁸ that miscibility gaps replace the MPB and the paraelectric to ferroelectric transition lines of the diffusionless phase diagram given in ref.¹ (which would be valid only if the cooling rate significantly exceeds the diffusion rate of Ti and Zr atoms). The analysis was restricted to temperatures above 420 K²⁸, although very similar conclusions should be valid at lower temperatures. Usually the solubility gap increases with decreasing temperature. In the present case the solubility gap and finite atomic diffusion rate would imply that system minimizes its free energy by segregating into two different phases possessing different compositions and crystal symmetries. Although it is probable that the equilibrium situation is not necessarily reached through standard sample preparation techniques, tendency towards two-phase co-existence is apparent in the vicinity of the MPB.

For simplicity we assume, based on a vast number of experimental studies, that the distribution of Zr and Ti is essentially random. For discussion purposes, we further assume that the spatial composition can be divided into two parts: (i) differences between the average compositions of grains, consisted of domains and (ii) composition variation within a domain. To quantify the meaning of spatial composition variation within a domain we assume that the distribution of Zr and Ti obeys the binomial density function with probabilities $p = x$ and $q = 1 - p$ that the B -cation site is occupied by Zr and Ti ion, respectively (the solubility gap would further enhance the spatial composition variation). This approximation provides a microscopic explanation for the two phase co-existence observed in the vicinity of the MPB and is consistent with the idea that Cm phase serves as a transitional phase between rhombohedral and tetragonal phases. To see this, we consider the case of PZT with $x = 0.50$: if we divide a large domain (say, with dimensions of the order of 1 μm) to cubes containing N primitive cells, roughly $2/3$ of the cubes contain $N_{Zr} = xN$ Zr ions with

$Np - \sqrt{Npq} \leq N_{\text{Zr}} \leq Np + \sqrt{Npq}$. If we now take the cube edge to be 10 nm (approximately corresponding to the volumes studied by TEM and ED techniques), almost 1/3 of the cubes have $x < 0.49$ or $x > 0.51$ (for large values of N binomial distribution can well be approximated by a Gaussian distribution). Spatial composition variation is the probable origin explaining why some domains are rhombohedral, whereas some are monoclinic. In a transition region (compositions between well established rhombohedral and tetragonal regions) Cm phase serves as a transition bridge. The idea of an inhomogeneous distribution of Zr and Ti ions is also consisted with the TEM and ED observations according to which there is a rather large spatial variation in ED patterns as discussed above. Surface phenomena are sensitive to local distortions. It is the feature of the binomial distribution that the variance is largest at around MPB composition ($p \approx q$) and is zero only for pure PbTiO_3 and PbZrO_3 . This is seen from the line widths which increases with increasing x when $0 \leq x \leq 0.50$. This is supported by an atomic pair distribution function analysis carried out for PZT powders with $x = 0.40, 0.52$ and 0.60^{29} : the MPB is a crossover point with maximum disorder. It is also important to note that even if the average composition of different grains would be exactly the same, the spatial variation is sufficient to generate domains with different symmetries. In practice, some composition variation in average compositions of different grains exists. Also the composition of grain boundaries is expectably different from the inner parts. The most important factor behind the two-phase 'co-existences' is probably related to the differences in average compositions of different domains: the domains with larger Zr content can entirely transform to rhombohedral phase, while it looks that the phase transformation cannot be completed in those domains containing larger amount of Ti but is frozen to Cm phase. We note that Cm phase was interpreted to relieve the stress which otherwise would be generated due to the *interacting* rhombohedral and tetragonal domains in ref.³⁰. From this point of view it is not a surprise that the Bragg reflections of the Cm phase are much wider than those of the $R3c$ phase.

On the other hand, if one could prepare an ordered PZT sample with $x = 0.50$, Cm phase might not be stable. To see this, we note that in the case of ordered PZT with $x = 0.50$ the Zr/Ti distribution is homogeneous in the primitive cell scale and any deviation from this order results in less homogeneous distribution. Correspondingly, there are no Zr rich or deficient areas and in this sense also the mechanism favouring Cm would be missing: if there are no local distortions due to the spatial composition variation, there likely are no domains with different symmetries (at least not so abundant as the experiments reveal), which in turn implies that there is no need for a phase serving as a bridge between rhombohedral and tetragonal phases. This might be important for a very small grain size powders where most of the grains would be consisted of one domain. Experimentally the

two extrema cases, perfect disorder and order, can easily be distinguished by x-ray or neutron diffraction techniques. As the studies dedicated to double perovskites show, ordering is clearly seen from the superlattice reflections in x-ray (for instance, see ref.³¹ where polymerized complex method was used to prepare Ba_2MnWO_6 double perovskites) and neutron powder diffraction patterns (see, e.g.,³²). Also Raman spectra are consisted with the observed diffraction patterns^{33,34}. As the numerous studies show the difference in ionic radii (and, to a lesser extent, charge) does not provide sufficient driving force an ordered structure. Although it may not be possible to prepare ordered bulk PZT samples the problem can be approached by computational techniques. Finite temperature Monte Carlo simulations carried out for PZT with a broad range of x and random distribution of Zr and Ti in the B -cation site yielded a phase transition sequence $P4mm \rightarrow Cm \rightarrow R3m^{35}$ (no interaction between different domains was incorporated in this study). Virtual crystal approximation (VCA, where Zr and Ti ions are replaced by the same fictitious average atom) does not reveal a Cm phase³⁵. It is an open question if VCA could reproduce Cm phase when the interaction between domains is taken into account. After all, Cm phase always co-exists with rhombohedral phase. The two-phase co-existence in the vicinity of the MPB has proven to be very puzzling and sometimes one can find reports according to which an 'ideal' sample preparation route could yield single phase samples. Recently, an equilibrium phase diagram satifying the Gibbs phase rule was given in ref.²⁸. The essential result was that, by the Gibbs phase rule, the single-phase fields on the phase diagram must be separated by two-phase regions (and Cm phase is by no means an exception)²⁸. According to ref.¹⁰, the flat energy surface near the rhombohedral phase may be the most important factor for high piezoelectric constant materials. As the co-existence suggests, this seems to be the case in PZT system.

III. ANISOTROPIC LINE BROADENING.

The anisotropic line broadening was ascribed to a 'microstrain' (*i.e.*, Zr substitution for Ti creates local strains which in turn contributes to the hkl -dependent line broadening)¹⁷. This is also enhanced by the spatial composition variation which further enhances the anisotropic line broadening. In addition, rather strong intensity is commonly observed between the $h00$ and $00l$ with $h = l$ Bragg reflections, which was assigned to locally disordered regions in the vicinity of the domains walls in ref.⁶. Especially at room temperature it is practically impossible to assign a precise structural model for this phase, since it is not well crystallized. It might also be a precursor phase which at higher Zr contents evolves into a rhombohedral phase. This interpretation was given to the data collected on PHT powders, see Fig. 4 in ref.¹⁹. Nevertheless, scattering from this phase adds

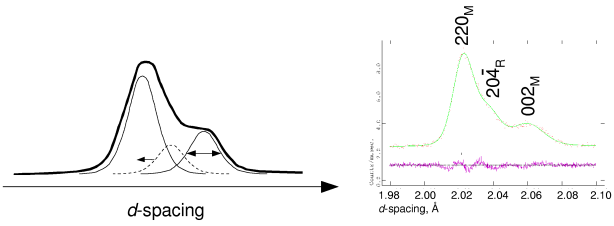


FIG. 1: Left panel: Schematic illustration of the way how the neglect of anisotropic line broadening affects the position of the rhombohedral peaks: once the rightmost peak broadens, it pushes the rhombohedral peak (middle) towards smaller d -spacing. Right panel: Observed and computed high resolution neutron powder diffraction profile collected on PZT with $x = 0.53$ at 4 K. Pseudo-cubic 200 reflection region is shown. Note that the 002_M peak (Cm phase) at around 2.06 \AA is significantly broader than the 220_M (Cm phase) peak at around 2.02 \AA . Now, the position of the rhombohedral 204_R peak depends on the way the line broadening is taken into account. Figure adapted from ref.³⁶

intensity to certain diffraction peaks, which in practise also contributes to an asymmetric line broadening (as it is not possible to unambiguously separate it: it is the sum from different contributions what one observes in the case of powder diffraction). For example, the larger and smaller d -spacings sides of the pseudo-cubic 200 and 002 reflections, respectively, seem to gain intensity. Particular care is necessary once this phase is modelled and generally one might do better by collecting data on samples with different Zr contents and at different temperatures.

Although a reasonable structure refinement for medium resolution data collected on PZT samples with $x \leq 0.50$ could be obtained using a lineshape which ignores anisotropic line broadening, the situation was quite different for high resolution facilities, particularly once the data was collected on two phase samples. In such a case it was essential to use an appropriate profile function. *Now, if the anisotropic line broadening is neglected*, the fit in the case of certain weak peaks becomes slightly worse (as was observed to be the case of weak superlattice reflections, which are less weighted in the refinements). The reason for this is illustrated in Fig. 1: in order to improve the fit corresponding to the strong pseudo-cubic 200 reflections, during the refinement the position of $R3c$ reflection is shifted toward higher d -spacings, which in turn resulted in a small shift of the weak peaks at 2.44 and 1.06 \AA . The anisotropic line broadening was not limited to the d -spacing at around 2 \AA , and similar mechanism was seen at other d -spacings. A structural model which reduces the symmetries to 'model' the hkl -dependent line broadening takes local disorder into account incorrectly, since in this way the disorder is assigned to be periodical, obeying the space group symmetry.

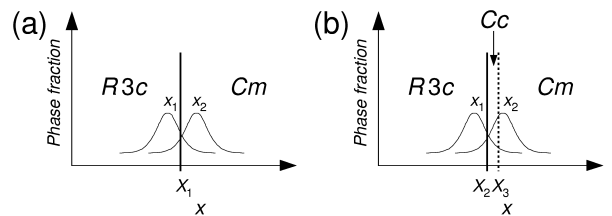


FIG. 2: The consequences of the spatial composition variation (at fixed temperature and pressure) in the case of two samples with average compositions x_1 and x_2 in the vicinity of (a) the phase boundary separating $R3c$ and Cm phases (at X_1) and (b) two phase boundaries separating $R3c$ and Cc (at X_2) and Cc and Cm phases (at X_3). Figure adapted from ref.³⁶

IV. TWO-PHASE MODELS

A. $\text{Pb}(\text{Zr}_{0.52}\text{Ti}_{0.48})\text{O}_3$ and $\text{Pb}(\text{Zr}_{0.53}\text{Ti}_{0.47})\text{O}_3$ samples

In the context of low-temperature phases the role of spatial composition variation was discussed in refs.⁴ and¹⁷. The room- and low-temperature crystal symmetry of Zr rich PZT ceramics is $R3c$ ^{3,17,37}, except for the compositions with $x \approx 1$ ³⁸. The room temperature symmetry of PbZrO_3 is $Pbam$ ^{39,40}. Since spatial composition variation cannot be completely eliminated, there must exist two phases in the vicinity of MPB. Fig. 2 (a) illustrates the consequences of spatial composition variation in the vicinity of MPB at low temperature. To allow the existence of Cc phase necessitates that there should be a narrow region in the $x - T$ plane where this phase is stable or metastable. Now, if we were to explain the existence of Cc phase, two phase boundaries located somewhere between $0.52 \leq x \leq 0.54$ should be assumed to exist, see Fig. 2 (b). This in turn, once the spatial composition variation is taken into account, leads to three phase 'co-existence'. The simplest $Cm + R3c$ model (corresponding to Fig. 2 (a)) was preferred in refs.^{4,17}, since it was able to explain the experimental observations in simplest terms. At low temperature (4 K¹⁷ or 10 K⁴) the phase fraction of the Cm phase was monotonically decreasing with x increasing from 0.52 to 0.54, which in turn implies that two-phase 'co-existence' is predominantly due to the spatial composition variation⁴¹.

It is worth to point out that the model proposed in ref.¹¹ was ruled out also in a recent paper, see the last paragraph in ref.⁴². After all, the only difference between $Cm + R3c$ model and $Cm + Cc$ model proposed in ref.⁴² is that $R3c$ symmetry was used (corresponding to two lattice parameters and four atomic coordinates) instead of the Cc symmetry (corresponding to four lattice parameters and twelve atomic coordinates, although constraints were used to decrease refinable parameters in ref.⁴²). Now, Cc is a subgroup of $R3c$ space group. Since no superlattice reflections characteristic only to Cc phase

were observed (such should appear at large d -spacing region, if symmetry is lowered from $R3c$ to Cc), $R3c$ symmetry was favoured in ref.⁴. This allowed considerably simpler structural model: one is tempted to ask how much can be gained by first decreasing the symmetry from $R3c$ to Cc and then decreasing the number of refinable parameters by introducing constraints. This issue is discussed on a more general ground in ref.⁴³. In ref.⁴² the use of Cc phase was largely based on the TEM and ED observations⁴⁴ according to which superlattice reflections, which were inconsistent with $R3c$ symmetry, were observed at low temperature. This observation is consistent with the observations reported in ref.²⁴ but the interpretation is entirely different. Now, it would be interesting to consider: (i) similar possibilities as were given in ref.²⁴ (summarized above), and (ii) if the observed features are only characteristic to TEM samples (layers with thickness between 5 and 100 nm were studied and it was further stated that the size distribution of Cc phase ranged between 3 to 10 nm⁴⁴). This is contrasted by the observation according to which the line widths of $R3c$ phase were much narrower than those of Cm phase¹⁷. Neither of the phases was in a form of 'nanoparticles'. It would also be interesting to see how large octahedral tilts are necessary to 'reproduce' the ED patterns, including those superlattice reflections which were taken as an evidence for Cc symmetry, since they were not observed by NPD studies. We note that $Cc + Cm$ and $Cm + Cc$ models, given in refs.¹¹ and⁴² respectively, are completely different (and mutually exclusive): they present models where Cm and Cc symmetries were swapped. Now, this type of space group swapping results in entirely different structural parameters and phase fractions. Needless to say, this has nothing to do with composition variation or differences in crystallite sizes, see also related discussion in ref.⁴⁵. Despite the increased number of refined parameters, the residuals were still rather high and the differences between different models compared in ref.¹¹ were marginal. For instance, R_{exp} was lowest for the $Cm + R3c$ model which was rejected in ref.¹¹. As discussed in the next section, the model given in ref.¹¹ does not assign octahedral tilts to a correct phase. In contrast, the models proposed in refs.⁴ and⁴² assigned octahedral tilts to the same phase. In the case of the data shown in ref.¹¹ the intensity of the peak(s) at around 1.06 Å was barely above the noise level and the $Cc + Cm$ model assigns more reflections than there are data points in this region. Thus these reflections do not provide justification for the use of Cc phase.

In addition, some reports claimed that dielectric measurements gave support to Cc phase (for example, see ref.¹³). Although these types of measurements might be useful once phase transitions in single phase samples are studied, not too much emphasis should be put on data collected on multiphase samples. In this context we note that the samples studied in refs.⁴⁶ and⁴⁷ contained a non-identified impurity phase(s), as was revealed by the peaks at around 28 and 35 two-theta degrees (corresponding to

d spacings 3.18 Å and 2.56 Å, respectively), in addition to the aforementioned two-phase co-existence. This implies that the composition was not well known and thus the possibility of compositional and structural inhomogeneities should be kept in mind. Although this non-perovskite phase was well resolved, it was not included in the Rietveld refinement model considered in ref.⁴⁶, which in turn results in an error in the structural parameters of the perovskite phase(s). This is likely related to the fact that the diffraction pattern shown in ref.⁴⁶ (reported to have $x = 0.52$) is reminiscent to the diffraction pattern with $x = 0.53$ shown in ref.⁴. In contrast, the diffraction pattern with $x = 0.52$ given in ref.⁹) and the diffraction pattern of the $x = 0.52$ sample reported in refs.⁴² and^{5,6} were reminiscent.

B. $\text{Pb}(\text{Zr}_{0.54}\text{Ti}_{0.46})\text{O}_3$ sample

The anisotropic line broadening and the absence of the superlattice reflection evidencing Cc symmetry in PZT powders with $x = 0.52$ and $x = 0.53$ provided a motivation to carry out a subsequent study using a high resolution NPD instrument¹⁷. To model the peak profiles, GSAS⁴⁸ lineshape 4 by Stephens⁷ was used in this study. In addition, Zr content was slightly increased to $x = 0.54$ ¹⁷ (although it was possible to fit *all* reflections using the $Cm + R3c$ model also in the case of $x = 0.52$ and $x = 0.53$ samples). This allowed a more reliable refinement and symmetry identification to be done by studying the *changes in phase fractions versus temperature*. Importantly, for these compositions it has been found that oxygen octahedra tilts increase with increasing x (see ref.³) and decreasing temperature (this feature is discussed in refs.⁴⁹ and⁴). We also note that previously Cc was proposed to be a space group symmetry corresponding to high isotropic pressure⁵⁰, whereas the present review concentrates on the determination of space group symmetries versus composition and temperature at ambient pressure. Now, PZT sample with $x = 0.54$ provided a test for clarifying which phase is the preferred one at low temperature. This is of particular interest also from the point of view of *ab initio* computations dedicated for PZT according to which the largest piezoelectric d_{33} coefficients are found to be large namely in the rhombohedral side of the MPB: much smaller values were found in the tetragonal side of the MPB⁵¹. These observations are consistent with the experimental observations on PZT⁵² and $\text{Pb}(\text{Zn}_{1/3}\text{Nb}_{2/3})\text{O}_3\text{-PbTiO}_3$ (PZN-PT) and $\text{Pb}(\text{Mg}_{1/3}\text{Nb}_{2/3})\text{O}_3\text{-PbTiO}_3$ (PMN-PT)⁵³ (the two latter systems also possess MPB separating rhombohedral and tetragonal phases). The NPD data in ref.¹⁷ suggests the following phase transition sequence with decreasing temperature in the vicinity of MPB: $Pm\bar{3}m \rightarrow P4mm \rightarrow Cm \rightarrow R3m \rightarrow R3c$ where adjacent groups have a group-subgroup relationship. Due to the composition variation some domains undergo the same phase transition sequence at higher (Zr richer) or lower

(Ti richer) temperatures. This sequence demonstrates the role of *Cm* phase linking *P4mm* and *R3m* phases. The co-existence of the rhombohedral and *Cm* phase is consistent with the idea that they are energetically almost as favourable and rather small changes in temperature, pressure or an applied electric field can transform *Cm* phase to rhombohedral phase. First-principles computational study revealed that the electric field induced phase transformation sequence with an increasing applied electric field was found to be reversed when the field was released⁵¹, whereas the same was not found experimentally in ref.⁵⁴. This different behaviour was attributed to defects³⁵: the model used in *ab initio* computations was defect free, whereas in practice defects cannot be completely eliminated.

As is seen from Fig. 1 in ref.¹⁷, once the crystals are compressed with decreasing temperature, the *R3c* phase was favoured and *Cm* phase did not transform to *Cc* phase, in strong contrast with the model proposed in ref.¹¹). We note that the volume of the *R3c* phase grows with decreasing temperature (for instance, see Fig. 1 in ref.¹⁷). Thus, no evidence was found for the *P4mm* \rightarrow *Cm* \rightarrow *Cc* phase transition sequence. When the oxygen octahedra had almost no chance to contract, they were rotated to opposite directions along the pseudo-cubic 111 axis (tilt system $a^-a^-a^-$). This tilt results in a decrease of the volume of cuboctahedra around Pb ions. Changes evidencing *Cc* symmetry (and the corresponding tilt system) were not observed. *Indeed, the phase fraction of Cm phase (which was assigned to Cc symmetry in ref.¹¹) decreased with decreasing temperature, whereas R3c phase fraction significantly increased with decreasing temperature.* This can be confirmed by a naked eye observation of the diffraction patterns in Fig. 1 in ref.¹⁷, although the results of refinements were also given. The intensity of the peak at around 1.06 Å was increasing with decreasing temperature, which further confirmed that its origin is the phase assigned to *R3c* phase. Also the peak at around 1.06 Å was well fit by *R3c* symmetry. In other words, in ref.¹¹ *Cc* phase was used to model the Bragg reflection from the pseudo-tetragonal phase and also the superlattice reflections. Thus, *Cc* symmetry was used to model Bragg peak from two distinct phases, which is not correct. However, the temperature and composition dependence clearly show that when the phase fraction of *Cm* phase decreased, the intensity of the superlattice reflection was increasing together with the phase fraction of *R3c* phase. This behaviour is consistent with the composition variation: the distortion (monoclinic or rhombohedral) and the volume of the distortion depend on average composition and temperature.

V. BOND-VALENCE SUMS AND ION VALENCES

Computations of bond valence sums (BVS) provides a way to test whether the bond lengths are reasonable. Al-

though it is not sensitive for minor changes in symmetry, unless bond lengths are altered, it has proven to be useful for confirming the effect of the proposed Pb, Zr and Ti ion displacements⁴. Namely, if Pb ions are constrained to be located in their ideal positions in the case of *P4mm* phase, the Pb ion valence would be $\approx +1.8$, whereas it is quite close to the nominal valence +2 once Pb ions are allowed to be displaced towards $\langle 110 \rangle$ directions. This is actually rather general tendency for Pb ion and occurs in rhombohedral phases. This is quite plausible since the cuboctahedra is so large that if Pb ion would occupy its centre, it would result in valence deficient Pb ions. Thus, by forming four short bonds with oxygen more reasonable valence values for Pb are achieved. Similarly, the average *B*-cation valence $v(B_{av}) = xv(\text{Zr}) + (1-x)v(\text{Ti})$ was +4 when Zr and Ti ions were allowed to have different fractional coordinates. In the case of the tetragonal PZT it was demonstrated that if one insists to constrain the fractional coordinates to be the same, no Wyckoff 1*b* position in the unit cell would correspond to the nominal valence +4. It also worth to point out that if Pb ions are constrained to be at the 1*a* site symmetry position Pb atomic displacement parameters (ADP) are very large. On the other hand, by constraining the *B* cations to have the same fractional coordinates yielded negative ADP values. Allowing Pb ions to be displaced towards $\langle 110 \rangle$ directions and Zr and Ti ions to have different fractional *z*-coordinates resulted in physically reasonable ADP values. From this point of view it was important to check the validity of the structural models by confirming that both anomalous valence and ADP values can be eliminated by the same structural model. Oxygen valences in PZT systems were close to their nominal valence value -2. Also oxygen ADP values were reasonable. Thus, as far as NPD studies are considered, it is a decent approximation to assume oxygen octahedra to fullfil the requirements of space group symmetry, in contrast to the case of cation positions. This also implied that it was not necessary to invoke the plausible mechanism, the expansion of Zr octahedra and contraction of Ti octahedra, to correct the anomalously large Zr and small Ti valences in the structural models used to model the NPD data.

BVS were found to be consistent with the observed phase transition sequences so that reasonable valence values for each ion were obtained also in the case of the *Cm* and *R3c* phases. The relationship between the oxygen octahedra and cuboctahedra volumes and octahedra tilts were pointed out in ref.⁴⁹. Namely, *R3c* symmetry allows oxygen octahedra tilt, which means that the volume of oxygen octahedra increases with increasing tilt angle. This in turn allows the valence of each ion to be close to their nominal values. The same is not possible in the case of *R3m* symmetry and thus the observed oxygen octahedra tilts versus temperature and *x* seen in the case of PZT samples with *x* = 0.52 and *x* = 0.53 are consistent with the 'constraints' set by nominal valences⁴. In many ways similar findings, based on density functional theory computations carried on PZT modelled with large

supercells, were reported in ref.⁵⁵. Perhaps the most essential difference between the typical Rietveld refinement models and supercell models for PZTs is that the space group symmetries used in the latter approach allow different size oxygen octahedra for Zr and Ti, whereas they are constrained to be the same in Rietveld refinements (one actually replaces both Zr and Ti by a 'pseudo-atom' whose scattering length (NPD) or cross section (X-ray diffraction) is a weighted average over Zr and Ti ions). This explains why the individual bond-valences for Zr and Ti were found to be close to their nominal values in the case of the supercell computations⁵⁵. In this sense it is surprising to see that both approaches support the idea that oxygen position do not suffer from local distortions to the extent cation positions do.

VI. CONCLUSIONS

The pitfalls related to the modelling of the crystal structures of PZT ceramics with different compositions and at different temperatures were reviewed. The role of the spatial composition variation, resulting in two-phase 'co-existence' in the vicinity of the phase boundaries and anisotropic line broadening, were reviewed. The conditions set to sample preparation, powder diffraction instrument and line shape were addressed. Focus was put on the structure analyses on PZT ceramics with compositions in the vicinity of the morphotropic phase boundary (MPB). Recent studies pointed out that the two-phase co-existence in the vicinity of the phase boundary is a thermodynamical necessity in PZT system and further is very crucial for the high electromechanical coupling coefficients observed in MPB compositions. Two different approaches for modelling the two-phase structures of PZT ceramics with compositions corresponding to the MPB

were identified. The first is a method where space group symmetry was decreased so that both local and average crystal symmetries were modelled, whereas the second method was based on the highest space group symmetry compatible with the observed Bragg reflections and where local distortions were taken into account by selecting an appropriate line shape. Recently published $Cm + Cc$ and $Cc + Cm$ structure models were compared with $Cm + R3c$ model where anisotropic line shapes were used. Whereas $Cm + R3c$ model is a higher symmetry version of $Cm + Cc$ model, $Cc + Cm$ model was shown to be inapplicable. Once the local distortions, resulting in anisotropic line broadening, are correctly taken into account, we do not find support for $Cm + Cc$ model. Instead we found that $Cm + R3c$ model describes all Bragg peaks and their intensities well. It was further shown that the $Cm + R3c$ model is consistent with the structural features observed at other compositions and temperatures, which is particularly important in the vicinity of the phase boundary. Also issues related to the effects of a finite sample size used in transmission electron microscopy and electron diffraction studies were discussed and it was pointed out that while locally ordered areas may occur in nanosize samples they frequently do not appear in bulk samples. Thus, the same structural model might not apply for nanoscale and bulk samples. Connection between the structural parameters and piezoelectric properties were discussed in light of the recent computational studies.

Acknowledgments

J. F. is grateful for the Academy of Finland for financial support (Project numbers 207071 and 207501).

* Electronic address: jfr@fyslab.hut.fi

- ¹ B. Jaffe, W. R. Cook and H. Jaffe, *Piezoelectric Ceramics*, (Academic Press, London, 1971).
- ² A. M. Glazer, P. A. Thomas, K. Z. Baba-Kishi, G. K. H. Pang and C. W. Tai. *Phys. Rev. B* **70**, 184123 (2004).
- ³ D. L. Corker, A. M. Glazer, R. W. Whatmore, A. Stallard, and F. Fauth. *J. Phys. Condens. Matter* **10**, 6251 (1998).
- ⁴ J. Frantti, S. Ivanov, S. Eriksson, H. Rundlöf, V. Lantto, J. Lappalainen, and M. Kakihana. *Phys. Rev. B* **66**, 064108 (2002).
- ⁵ B. Noheda, D. E. Cox, G. Shirane, J. A. Gonzalo, L. E. Cross and S-E. Park. *Appl. Phys. Lett.* **74**, 2059 (1999).
- ⁶ B. Noheda, J. A. Gonzalo, L. E. Cross, R. Guo, S-E. Park, D. E. Cox, and G. Shirane. *Phys. Rev. B* **61**, 8687 (2000).
- ⁷ P. W. Stephens. *J. Appl. Crystallogr.* **32** 281 (1999).
- ⁸ A. Leineweber and E. J. Mittemeijer. *J. Appl. Cryst.* **37** 123 (2004).
- ⁹ J. Frantti, J. Lappalainen, S. Eriksson, V. Lantto, S. Nishio, M. Kakihana, S. Ivanov, and H. Rundlöf. *Jpn. J. Appl. Phys.* **39**, 5697 (2000).

¹⁰ H. Fu and R. E. Cohen. *Nature* **403**, 281 (2000).

¹¹ R. Ranjan, A. K. Singh, Ragini, and D. Pandey. *Phys. Rev. B* **71**, 092101 (2005).

¹² For clarity we note that this report was based on previously published neutron powder diffraction data. Same powder diffraction pattern was given in refs.¹³ and¹⁴, where it was modelled by Pc and Cc symmetries, respectively (so that they were both single phase models which actually seems to be the origin of the problems in their structural models).

¹³ R. Ranjan, S. K. Mishra, D. Pandey and K. Kennedy. *Phys. Rev. B* **65**, 060102 (2002).

¹⁴ D. M. Hatch, H. T. Stokes, R. Ranjan, Ragini, S. K. Mishra, D. Pandey, and B. J. Kennedy, *Phys. Rev. B* **65**, 212101 (2002).

¹⁵ In this paper we use both terms 'locally ordered regions' and 'local distortions' to emphasize the difference between ordered regions possessing short range order in cations shifts in a scale of a few unit cells and deviations from the average symmetry lacking any short range order. An example of the former is given in refs.² and³, whereas inho-

mogeneous distributions of different size *B*-cations result in spatial variation of the lattice parameters.

¹⁶ One can make the difference between measured and calculated diffraction intensities arbitrarily small by simply using space group *P1* and increasing the primitive cell size until the difference is below the desired value.

¹⁷ J. Frantti, S. Eriksson, S. Hull, V. Lantto, H. Rundlöf, and M. Kakihana. *J. Phys.: Condens. Matter* **15**, 6031 (2003).

¹⁸ Y. Ikeuchi, S. Kojima and T. Yamamoto. *Jpn. J. Appl. Phys.* **36**, 2985 (1997).

¹⁹ J. Frantti, Y. Fujioka, S. Eriksson, S. Hull and M. Kakihana. *Inorg. Chem.* 2005 **44**, 9267 (2005).

²⁰ J. Frantti, V. Lantto, S. Nishio and M. Kakihana. *Phys. Rev. B* **59**, 12 (1999).

²¹ J. Frantti, J. Lappalainen, S. Eriksson, V. Lantto, S. Nishio, M. Kakihana, S. Ivanov, and H. Rundlöf. *Jpn. J. Appl. Phys.* **38**, 5679 (1999).

²² J. Frantti, Y. Fujioka, S. Eriksson, V. Lantto, and M. Kakihana. *Journal of Electroceramics* **13**, 299 (2004).

²³ D. Viehland. *Phys. Rev. B* **52**, 778 (1995).

²⁴ J. Ricote, D. L. Corker, R. W. Whatmore, S. A. Impey, A. M. Glazer, J. Dec and K. Roleder. *J. Phys. Condens. Matter* **10**, 1767 (1998).

²⁵ K. Leung, *Phys. Rev. B* **67**, 104108 (2003).

²⁶ W. Cao and L. E. Cross. *Phys. Rev. B* **47**, 4825 (1993).

²⁷ M. V. Rane, A. Navrotsky and G. A. Rossetti, Jr. *J. Solid State Chem.* **161**, 402 (2001).

²⁸ G. A. Rossetti, Jr., W. Zhang and A. G. Khachaturyan. *Appl. Phys. Lett.* **88**, 072912 (2006).

²⁹ W. Dmowski, T. Egami, L. Faber and P. K. Davies. in *Fundamental Physics of Ferroelectrics-Eleventh Williamsburg Ferroelectric Workshop*, edited by R. E. Cohen (American Institute of Physics, Melville, NY, 2001), p. 33.

³⁰ V. Topolev and A. Turik. *J. Phys.: Condens. Matter* **13**, 771 (2001).

³¹ Y. Fujioka and M. Kakihana. *Trans. Mater. Res. Jpn.* **28**, 373 (2003).

³² A. K. Azad, S. Ivanov, S.-G. Eriksson, J. Eriksen, H. Rundlöf, R. Mathieu and P. Svedlindh. *Mater. Res. Bull.* **36**, 2215 (2001).

³³ Y. Fujioka, J. Frantti and M. Kakihana. *J. Phys. Chem.* **110**, 777 (2005).

³⁴ M. Liegeois-Duychaerts P. Tarte. *Spectrochim. Acta* **30A**, 1711 (1974).

³⁵ L. Bellaiche, A. García. *Phys. Rev. Lett.* **84**, 5427 (2000).

³⁶ J. Frantti. (2005-07-04) oai:arXiv.org:cond-mat/0504432.

³⁷ C. Michel, J. M. Moreau, G. D. Achenbach, R. Gerson, and W. J. James, *Solid State Commun.* **7**, 865 (1969).

³⁸ The situation might be different for a high pressure case or at low temperatures in the case of the Zr rich PZT (e.g., for $x \geq 0.60$) since the octahedral tilting allowed by *R3c* symmetry might no more be sufficient. If so, one could expect that this phase extends to a larger values of x . One may also speculate if symmetries allowing different octahedral tilts could be stabilized in the case of strained thin films.

³⁹ A. M. Glazer, K. Roleder and J. Dec. *Acta Cryst.* **B49** 846 (1993).

⁴⁰ D. L. Corker, A. M. Glazer, J. Dec, K. Roleder and R. W. Whatmore. *Acta Cryst.* **B53** 135 (1997).

⁴¹ Although spatial composition variation is mainly responsible for the two-phase co-existence and line broadening phenomena, other factors, such as crystal size, have an effect on line broadening and probably affect phase fraction estimations.

⁴² D. E. Cox, B. Noheda, and G. Shirane. *Phys. Rev. B* **71**, 134110 (2005).

⁴³ W. Massa. *Crystal Structure Determination*, (Springer-Verlag, Berlin, 2000), p. 157.

⁴⁴ B. Noheda, L. Wu and Y. Zhu. *Phys. Rev. B* **66**, 060103 (2002).

⁴⁵ B. Noheda and D. E. Cox. (2005-11-10) oai:arXiv.org:cond-mat/0511256.

⁴⁶ Ragini, R. Ranjan, S. K. Mishra, and D. Pandey, *J. Appl. Phys.* **92**, 3266 (2002).

⁴⁷ Ragini, S. K. Mishra, D. Pandey, H. Lemmens, and G. Van Tendeloo. *Phys. Rev. B* **64**, 054101 (2001).

⁴⁸ A. C. Larson and R. B. Von Dreele *General Structure Analysis System*, LANSCE MS-H805, Los Alamos National Laboratory, Los Alamos, NM 87545 (2000).

⁴⁹ N. W. Thomas and A. Beitollahi. *Acta Crystallorg., Sect. B: Struct. Sci.* **50**, 549 (1994).

⁵⁰ J. Rouquette, J. Haines, V. Bornand, M. Pintard, Ph. Papat, W. G. Marshall, and S. Hull. *Phys. Rev. B* **71**, 024112 (2005).

⁵¹ L. Bellaiche, A. García. *Phys. Rev. B* **64**, 060103 (2001).

⁵² X. Du, J. Zheng, U. Belegudu and K. Uchino. *Appl. Phys. Lett.* **72**, 2421 (1998).

⁵³ S.-E. Park and T. Shrout. *J. Appl. Phys.* **82**, 1804 (1997).

⁵⁴ B. Noheda, D. E. Cox, G. Shirane, S.-E. Park, L. E. Cross and Z. Zhong. *Phys. Rev. Lett.* **86**, 3891 (2001).

⁵⁵ I. Grinberg, V. R. Cooper and A. M. Rappe. *Phys. Rev. B*, 144118 (2004).